

# Constraining the Drag Coefficients of Meteors in Dark Flight

R. T. Carter • P. S. Jandir • M. E. Kress

**Abstract** Based on data in the aeronautics literature, we have derived functions for the drag coefficients of spheres and cubes as a function of Mach number. Experiments have shown that spheres and cubes exhibit an abrupt factor-of-two decrease in the drag coefficient as the object slows through the transonic regime. Irregularly shaped objects such as meteorites likely exhibit a similar trend. These functions are implemented in an otherwise simple projectile motion model, which is applicable to the non-ablative dark flight of meteors (speeds less than  $\sim 3$  km/s). We demonstrate how these functions may be used as upper and lower limits on the drag coefficient of meteors whose shape is unknown. A Mach-dependent drag coefficient is potentially important in other planetary and astrophysical situations, for instance, in the core accretion scenario for giant planet formation.

**Keyword** meteorite · drag

## 1 Introduction

The scientific value of meteorites motivates many efforts to recover them quickly. To expedite the collection of meteorites resulting from observed fireballs, one must better constrain where they may have landed. Given an object's instantaneous position and velocity (in three dimensions), its mass (as inferred from deceleration) and its drag coefficient, its landing site can be constrained.

In recent years, detailed observations of meteors have been made by the European Fireball Network [16] [18], the Desert Fireball Network [3], and the Southern Ontario Network [22], resulting in the recovery of many meteorites. These detection networks can measure a meteor's position and velocity with very high precision. The Neuschwanstein Bolide was observed by the European Fireball Network; its angle is constrained to  $\pm 0.07^\circ$ , the altitude to  $\pm 50$  m, and the speed to  $\pm 800$  m s<sup>-1</sup> [17] [19]. Information about the mass of the object can also be derived from observations [17].

Considering the high accuracy to which observables can be measured, the drag coefficient introduces most of the uncertainty in calculating the landing site of these observed meteors. Detailed analysis of the drag coefficients of meteorites is daunting because meteorites are irregularly-shaped objects, and thus have different drag coefficients, not only for each individual object but also for the infinite number of orientations each can assume as they tumble, spin and ablate during flight. Nevertheless, there has been much effort to determine the drag coefficient for meteorite-like shapes (e.g. [23] [10]). Several studies have used or derived constant values for drag coefficients (e.g. [5] [23] [10] [21]).

---

R. T. Carter

Department of Physics, University of Oregon, Eugene, OR 97403 USA. E-mail: rcarter2@uoregon.edu

P. S. Jandir, Department of Physics, University of California, Riverside, CA 92521 USA

M. E. Kress (✉), Department of Physics & Astronomy, San José State University, CA 95192 USA. E-mail: mkress@science.sjsu.edu

Mach number,  $M$ , is an object's speed relative to the local speed of sound. In Earth's atmosphere, the speed of sound depends on the square root of the temperature of air and thus is primarily a function of altitude. At sea level, the speed of sound is approximately 340 km/s. We derived empirical equations for the drag coefficient as a function of Mach number from the data available in the aeronautical engineering literature [9] [11] [12]. In these studies, the drag coefficients for spheres were measured up to Mach 10 and for cubes up to Mach 3. From these data, we derive functions for the drag coefficients  $C_D(M)$  for spheres and cubes. We use these two  $C_D(M)$  functions as lower and upper limits for the drag on a meteor. We note that drag coefficients dependent on Mach number have been used in meteor physics before, e.g. [6] and often define the drag coefficient as  $\Gamma$ , which is related to  $C_D$  via the relation  $\Gamma = 0.5C_D$ . Here, when we refer to the drag coefficient, we use the  $C_D$  convention.

In section 2, we present the  $C_D(M)$  functions for spheres and cubes, and explain how the equations of motion are solved. In section 3, we show how Mach-dependent drag affects the landing site for the idealized cases of spherical and cubic 'meteors.' We illustrate how the search area is smaller when using a  $C_D(M)$  whose limits are set by a sphere and cube, compared to a search area delimited with constant  $C_D$ . In section 4, we discuss how  $C_D(M)$  becomes increasingly important for meteors whose mass, velocity, altitude and entry angle cause them to spend more time at lower velocities where the drag coefficient varies the most. In section 5, we summarize our findings and discuss how a Mach-dependent drag coefficient may improve upon other planetary and astrophysical calculations.

## 2 Model

The drag coefficients for several regular shapes, including a sphere and a cube, have been experimentally measured over a wide range of Mach numbers [9] [11] [12]. In these ballistic range tests, pellets in the shape of spheres and cubes were shot out of high velocity guns. For all speeds, the drag coefficient for a cube is always about a factor of two greater than that for a sphere. However, spheres and cubes exhibit similar trends in  $C_D(M)$  (see Figure 1). At low speeds, the drag coefficient of a cube is 1.09 and that of a sphere is 0.46. These both almost double as the speed increases to Mach 1.5, and then they level off to 1.7 and 0.9 respectively, at high Mach numbers. Therefore, the Mach number has as much of an effect on drag coefficient as does the shape, when comparing spheres and cubes.

Using these experimental data, best fit functions were derived to estimate the drag coefficient of spheres and cubes as a function of Mach number (Figure 1). Both of these drag coefficient functions are piece-wise. At lower speeds,  $C_D$  depends on  $M^2$ , and the best fit functions are quadratic. In the supersonic ( $M > 1$ ) regime, the best fit functions are both a sum of two exponentials. The drag coefficient of a cube as a function of Mach number is

$$\begin{aligned} C_D(M) &= 0.60M^2 + 1.04, & 0 \leq M \leq 1.150 \\ C_D(M) &= 2.1e^{-1.16(M+0.35)} - 6.5e^{-2.23(M+0.35)} + 1.67, & M > 1.150 \end{aligned} \quad (1)$$

The drag coefficient of a sphere as a function of Mach number is

$$\begin{aligned} C_D(M) &= 0.45M^2 + 0.424, & 0 \leq M \leq 0.722 \\ C_D(M) &= 2.1e^{-1.2(M+0.35)} - 8.9e^{-2.2(M+0.35)} + 0.92, & M > 0.722 \end{aligned} \quad (2)$$

In the hypersonic regime, ( $M > 5$ ), the drag coefficient for a cube levels off to a constant value of 1.67. That of a sphere approaches 0.92. In general, the drag coefficients of simple shapes tend to

approach a constant value as Mach number increases. This tendency, known as Mach number independence, is well documented in aeronautics [2]. However, Mach number independence does not mean that models of meteors traveling at arbitrarily high Mach numbers should use a constant drag coefficient. At sufficiently high speeds, enough heat is generated to dissociate the air molecules surrounding a meteor. This changes the fluid properties of the air which, in turn, affects the drag coefficient [1]. Thus, our Mach-dependent drag coefficient is most applicable to a meteor's 'dark flight', which commences when a meteor's speed drops below Mach 10 [4] [20] [14]. At speeds greater than this, one must consider energy losses via radiation and ablation in the equations of motion. [7] [8]

We implement the Mach-dependent drag coefficients in a two-dimensional projectile motion calculation. Input parameters include the meteor's altitude, its velocity (speed and angle), its final (post-ablation) mass and the drag coefficient  $C_D(M)$  of the object. Our model uses the fourth order Runge-Kutta method to solve the differential equations of motion,

$$\frac{\partial^2 x}{\partial t^2} = -\frac{F_{D,x}}{2m} \left( \frac{\partial x}{\partial t} \right) \quad (3)$$

$$\frac{\partial^2 y}{\partial t^2} = -\frac{mg - F_{D,y}}{2m} \left( \frac{\partial y}{\partial t} \right) \quad (4)$$

where  $x$  is the horizontal position along the direction of flight,  $y$  is the vertical position of the bolide,  $m$  is the mass of the bolide,  $F_{D,x}$  is the force due to drag in the  $x$ -direction ( $= \frac{1}{2}C_D(M)\rho A \cos\theta v^2$ ) and likewise for the  $y$ -direction,  $v$  is the speed of the object,  $A$  is the cross-sectional area of the meteoroid,  $\theta$  is the angle of the velocity vector with respect to horizontal, and  $\rho$  is the density of air. Atmospheric density, temperature, and pressure are calculated as a function of altitude using the U.S. 1976 Standard Atmosphere [13]. We emphasize that this expression for the drag force is appropriate for an object that is in dark flight (velocity less than about Mach 10).

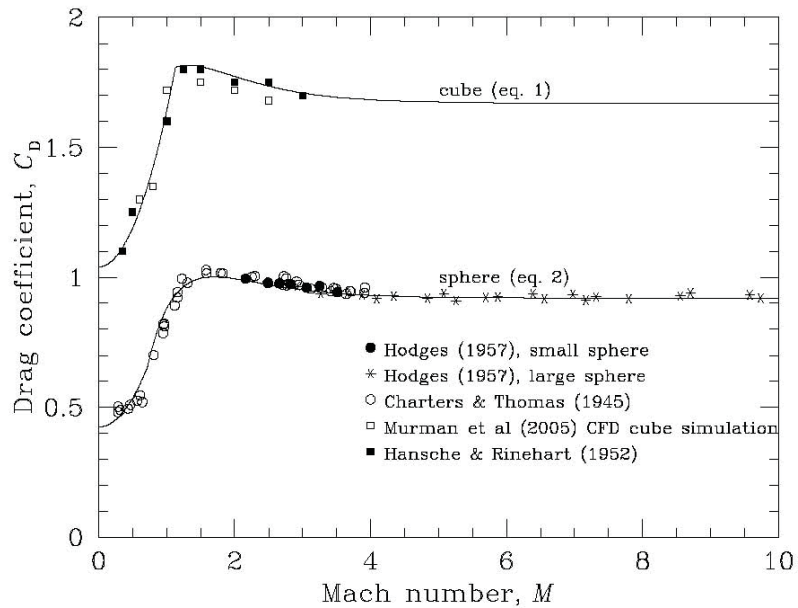


**Figure 1.** Drag coefficients as a function of Mach number for a sphere and a cube. Our best fit functions for a sphere and a cube (equations 1 and 2) are plotted along with experimental data [9] [11] [12]. Also shown are more current numerical results for a cube [15].

### 3 Results

We begin by applying the model to the idealized case of a sphere. This allows us to calculate the exact landing site, using our Mach-dependent drag coefficient for a sphere. We compare this to the landing position calculated using a constant low-Mach drag coefficient for a sphere of 0.464.

For the initial angle, speed, and altitude of this bolide, we use the values measured for the Neuschwanstein main body fragment as observed just before dark flight. We chose this meteor because its properties were very well measured by the European Fireball Network: studies of this event determined an angle of  $49.23^\circ \pm 0.07^\circ$  measured from the horizontal, a speed of  $3.1 \pm 0.8 \text{ km s}^{-1}$ , and an altitude of  $16.06 \pm 0.05 \text{ km}$  [19] [17]. The mass of the Neuschwanstein main body fragment is estimated to be 15 kg [17]. We will refer to these as the ‘Neuschwanstein parameters’ in the discussion that follows.

When the drag coefficient of this spherical meteor is kept constant at its low-velocity value of 0.464, the drag force is greatly underestimated. The sphere is predicted to land approximately 1880 m further downrange compared to the result obtained with the Mach-dependent drag coefficient given in Equation 1.

We did the same analysis for a cube-shaped meteor. The landing site computed with the Mach-dependent drag coefficient given in Equation 2 lands about 806 m further uprange than that calculated with a constant drag coefficient for a cube of 1.094. The cube is less affected because its greater drag causes it to spend more time with a  $C_D$  closer to its low-Mach value. The sphere, on the other hand, stays at high speeds longer, and thus spends more time with a  $C_D$  that is much greater than its low-Mach value. The more aerodynamically-shaped the object, the more important is the use of a Mach-dependent drag coefficient.

In Figure 2, we show the landing ellipses for a meteor coming in from the left. The landing ellipse is the area in which the resulting meteorite is likely to fall, and is determined by uncertainties in the meteor’s motion, shape and mass. This meteor has Neuschwanstein parameters as described above.

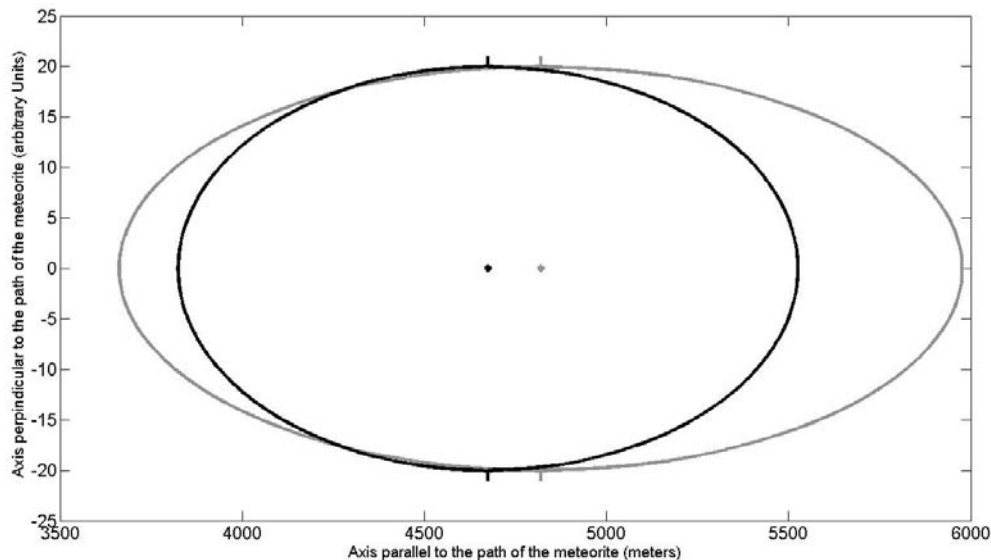


**Figure 2.** Landing ellipses for a meteor with Neuschwanstein parameters (see text). The length of the black ellipse is bound by the Mach-dependent drag coefficients  $C_D(M)$  for a sphere and cube (equations 1 and 2). The gray ellipse is bound by using a constant drag coefficient of 0.7 and 1.6. The centroid of the Mach-dependent calculation is shifted uprange by approximately 150 m; the area of the constant-drag ellipse is 1.36 times that of the  $C_D(M)$  ellipse.

The vertical axis of the ellipse is perpendicular to the meteor's velocity. Its units are arbitrary, determined in practice by crosswinds and uncertainty in the meteor's position and velocity. The horizontal axis is parallel to the meteor's flight. The gray ellipse is calculated with constant values for  $C_D$  and the black ellipse is calculated using our  $C_D(M)$  method. The points indicate the positions of the centroids of the ellipses.

The major axis of the constant  $C_D$  ellipse is determined by the low and high drag estimates for a meteor, 0.7 and 1.6, respectively. The value of 1.6 is that of a cube at high Mach numbers [23], which we assign to be the upper limit. A  $C_D$  of 0.7 is the low-Mach value from Ceplecha [6], which we use here as a lower limit on the drag coefficient.

The length of  $C_D(M)$  ellipse is bound by the  $C_D(M)$  functions for a sphere and cube (Equations 1 and 2). The centroid of the  $C_D(M)$  ellipse is shifted approximately 150 m uprange from the centroid of the constant-drag ellipse. The area of an ellipse is  $\pi ab$ , where  $a$  and  $b$  are the semi-major and semi-minor axes, and thus the ratio of the two areas is the ratio of the semi-major axes (given the same uncertainty in semi-minor axes). The area of the landing ellipse calculated using constant values for drag is about 1.36 times greater than the area of the one bound by our Mach-dependent drag coefficients for spheres and cubes.

## 4 Discussion

When using our Mach-dependent drag model to constrain the search ellipse for real meteors, the assumption is that the object will be less aerodynamic than a sphere and more aerodynamic than a cube. Our discussion here also implicitly assumes that the irregularly-shaped object will have a Mach-dependent drag coefficient that follows the same trend as that for spheres and cubes (i.e. a decrease in drag coefficient as the object slows through the transonic regime).

The Neuschwanstein bolide was a deeply-penetrating fireball that entered dark flight at an altitude of just over 16 km. Dark flight often begins at much higher altitudes. A recent example is the Bunburra Rockhole meteorite, which began dark flight at an altitude of 30 km [20]. In these types of falls, the altitude introduces more time for drag to operate, which means a substantially larger search area, regardless of what method is used to calculate it. Thus, constraining the search area even by 27% (from the example of the Neuschwanstein fireball) can be helpful to meteorite hunters.

We conducted an exploration of parameter space to determine what meteors would be most affected by our Mach-dependent drag coefficient. Not surprising, the Mach-dependent drag was more important for bolides that entered dark flight at higher altitudes and at shallower angles. The mass had a less dramatic effect: only for masses smaller than 1 kg did the landing ellipse change substantially. The speed also had an important influence on the landing ellipse. We show a plausible scenario in Figure 3, in which we constrain the landing site of a (non-ablating) meteor with a mass of 15 kg, at an altitude of 36 km, a speed of  $7.1 \text{ km s}^{-1}$ , and an angle of  $29^\circ$  measured from the horizontal. (We chose a velocity higher than the 3 km/s upper limit on the non-ablative phase of dark flight to force the meteor to spend more time in the hypersonic regime where  $C_D$  does not vary as much. Meteors with lower initial speeds will have more of their flight take place in the  $M < 5$  regime where the  $C_D$  varies significantly.) In this case, the areas of the landing ellipses calculated with the constant-drag method and our method have the same ratio (about 1.36). However, the centroid of the ellipse found with our method is about 1.4 km uprange, and this ellipse is no longer entirely contained within the constant-drag ellipse (see Figure 3).

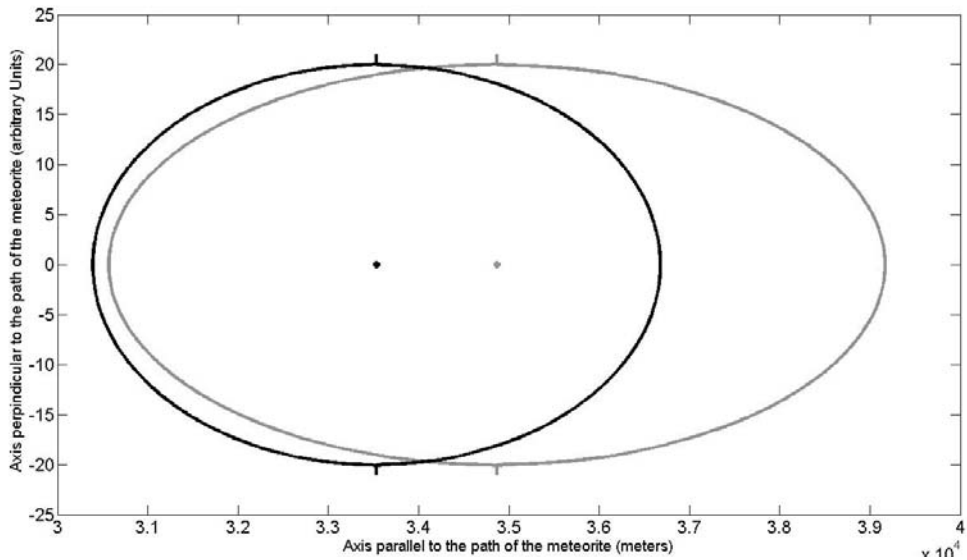


**Figure 3.** Landing ellipses for a hypothetical but plausible meteor. The length of the black ellipse is bound by the Mach-dependent drag coefficients  $C_D(M)$  for a sphere and cube (equations 1 and 2). The gray ellipse is bound by using a constant drag coefficient of 0.7 and 1.6. The centroid of the Mach-dependent calculation is shifted uprange by approximately 1400 m; the area of the constant-drag ellipse is 1.36 times that of the  $C_D(M)$  ellipse.

When a meteor has been observed and successfully recovered, one can empirically derive a constant drag coefficient that reproduces the known landing site. However, this technique has no predictive power. It is unlikely that the same constant  $C_D$  will work in a model of any other meteorite with different initial conditions, even if it has similar mass and shape. A difference in angle, speed, and starting altitude will affect the amount of time it spends in the high vs. low Mach/drag regimes. Instead, a Mach-dependent drag coefficient, similar to equations 1 and 2, can be derived for meteorites that have been recovered after observed falls.

## 5 Conclusions

The drag coefficient,  $C_D$ , is an important parameter in determining the landing site of observed meteors, but the value for  $C_D$  is notoriously elusive. Aerodynamic studies of regular shapes (spheres and cubes) reveal that an object's speed affects its drag coefficient as much as its shape does. This trend likely holds true for irregularly-shaped objects such as meteorites. All but the most oddly-shaped meteoroids likely have shapes such that their aerodynamic properties cause them to suffer less drag than cubes and more drag than spheres of the same mass traveling at the same speed.

We have derived functions for drag coefficients as a function of Mach number from experimental data for spheres and cubes. These functions can be readily implemented into any model for meteor trajectories that currently uses a constant value for the drag coefficient. Dark flight trajectories and landing ellipses were then computed using these drag coefficient functions, and compared to those computed using constant drag coefficients. The landing ellipses bound by spheres and cubes is smaller compared to those calculated using constant drag coefficients from 0.7 to 1.6. We also find that the centroids of the ellipses are shifted uprange, sometimes by more than 1 km.

More work must be done to understand the changes in drag coefficients due to the dissociation of air at the high temperatures generated around the incoming bolide. Accounting for this phenomenon is necessary in order to build a complete model of meteor flight. This issue has been explored by scientists in the field of aerothermodynamics, but has not yet been applied to meteor physics. Current studies in aeronautics may yield useful results for meteor scientists, for instance studies of irregular solids undergoing atmospheric entry (satellite wreckage and other space debris, e.g. [15]).

Finally, we anticipate other astrophysical and planetary applications of a Mach-dependent drag coefficient. For instance, the drag coefficient is an important factor in calculating the motion of planetesimals in gas-rich astrophysical disks such as the solar nebula, and also in the giant planet subnebulae. In these scenarios, the drag coefficient is assumed to be constant, usually 1 (e.g. [21]). Variable drag coefficients may have important consequences for the timescales for planet formation and for the coagulation of solids in planet-forming disks around other stars.

## Acknowledgements

The authors thank the US National Science Foundation for supporting RTC and PSJ via a Research Experience for Undergraduates grant to SJSU. MEK acknowledges support from the NASA Astrobiology Institute. We would also like to thank Gary Allen, Jeff Brown, Stuart Rogers, Jeff Hollingsworth, Laura Iraci, Prestin Martin, and Jeff Johnson for their suggestions for the manuscript and James Schombert, Scott Murman, Wendy Sullivan, Alejandro Garcia, Michael Kaufman, and Joshua Johnson for additional help.

## References

1. Anderson, J.D., *Fundamentals of aerodynamics*, McGraw-Hill, New York (2001)
2. Anderson, J.D., *Hypersonic and high-temperature gas dynamics*, American Institute of Aeronautics and Astronautics, Reston, Virginia (2006)
3. Bland, P.A., *Astron. Geophys.*, 45, 520 (2004)
4. Borovicka, J., Kalenda P., *Meteorit. Planet. Sci.*, 38, 1023 (2003)
5. Brown, P., Hildebrand, A.R., Green, D.W.E., Page, D., Jacobs, C., ReVelle, D., Tagliaferri, E., Wacker, J., Wetmiller, B., *Meteorit. Planet. Sci.*, 31, 502 (1996)
6. Ceplecha, Z., *Bull. Astron. Inst. Czechosl.*, 38, 222 (1987)
7. Ceplecha, Z., Borovicka, J., Elford, W.G., Revelle, D.O., Hawkes, R.L., Porubcan, V., Simek, M., *Space Sci. Rev.*, 84, 327 (1998)
8. Ceplecha, Z., ReVelle, O., *Meteorit. Planet. Sci.*, 40, 35 (2005)
9. Charters, A.C., Thomas, R.N., *J. Aeronautical Sci.*, 12, 468 (1945)
10. Gritsevich, M.I., Stulov, V.P., *Solar System Res.*, 42, 118 (2008)
11. Hansche, G.E., Rinehart, J.S., *J. Aeronautical Sci.*, 19, 83 (1952)
12. Hodges, A.J., *J. Aeronautical Sci.*, 24, 755 (1957)
13. Lewis, B., *The Complete 1976 Standard Atmosphere*, <http://www.mathworks.com/matlabcentral/fileexchange/13635-complete-1976-standard-atmosphere> (2007)
14. McCrosky, R.E., Posen, A., Schwartz, G., Shao, C.-Y., *SAO Special Report*, 336, 1 (1971)
15. Murman, S.M., Aftosmis, M.J., Rogers, S.E., *American Institute of Aeronautics and Astronautics*, 43, 1223 (2005)
16. Oberst, J., Molau, S., Heinlein, D., Gritzner, C., Schindler, M., Spurný, P., Ceplecha, Z., Rendtel, J., Betlem, H., *Meteorit. Planet. Sci.*, 33, 49 (1998)
17. Oberst, J., Heinlein, D., Kohler, U., Spurný, P., *Meteorit. Planet. Sci.*, 39, 1627 (2004)
18. Porubcan, V., Svoren, J., Husárik, M., Kanuchová, Z., *Contrib. Astron. Obs. Skalnaté Pleso*, 39, 101 (2009)
19. Spurný, P., Heinlein, D., Oberst, J., *Asteroids, Comets, Meteors*, ed: B. Warmbein, ESA Publications Division, Noordwijk, 137 (2002)

20. Spurný, P., Bland, P.A., Borovicka, J., Shrbeny, L., McClafferty, T., Singleton, A., Brevan, W. R., Vaughan, D., Towner, M.C., Deacon, G., 40th Lunar and Planetary Sciences Conf., 1498, 1 (2009)
21. Tanigawa T., Ohtsuki, K., Icarus, 205, 658 (2010)
22. Weryk, R.J., Brown, P.G., Domokos, A., Edwards, W.N., Krzeminski, Z., Nudds, S.H., Welch, D.L., Earth, Moon, Planets, 102, 241 (2008)
23. Zhdan, I.A., Stulov, V.P., Stulov, P.V., Turchak, L.I., Solar System Research, 41, 505 (2007)